

# Maxsim, software for the analysis of multiple axonal arbors and their simulated activation

Laurent Tettoni<sup>a</sup>, Patricia Lehmann<sup>a</sup>, Jean-Christophe Houzel<sup>b</sup>, Giorgio M. Innocenti<sup>a,\*</sup>

<sup>a</sup> *Institut d'Anatomie, 9 rue du Bugnon, 1005 Lausanne, Switzerland*

<sup>b</sup> *Laboratoire de Physiologie de la Perception et de l'Action, CNRS UMR9950, Collège de France, 11 Place Marcelin Berthelot, 75231 Paris Cedex 05, France*

Received 19 July 1995; accepted 2 August 1995

## Abstract

In order to analyze the structural organization of complex axonal arbors reconstructed from histological serial sections, and to investigate the functional implications of their geometrical properties, we developed software providing the following facilities: (1) direct importation of data files generated by a commercially available 3-D light-microscopic reconstruction system, including routine procedures for identification and correction of data acquisition errors; (2) real-time 3-D rotations of the arbors in the stack of serial sections; (3) multiple interactive display modes; (4) possibility of modifying diameter and/or connectivity of different branches; (5) simulation of the invasion of the arbor by a single action potential initiated at any chosen point, and visualization of spatio-temporal profiles of activation; (6) extraction of quantitative data converted to standard file formats compatible with available mathematical software. All these tools can be applied to single or multiple axons, individually or simultaneously. The software, called Maxsim, is a highly flexible C-written program running on graphical workstations using the UNIX operating system and X-Window environment.

*Keywords:* Axon; Computation; Morphology; Simulation; Computer method

## 1. Introduction

The analysis of axons is crucial for understanding the architecture of central nervous system connections and their function. Unfortunately, with a few exceptions, the analysis has been severely limited by the absence of techniques for visualizing terminal arbors of long axons completely and in detail. This situation has recently improved due to the use of new anterograde tracers such as *Phaseolus leucoagglutinin* (Gerfen and Sawchenko, 1984), biocytin (King et al., 1989) and dextran amines (Schmued et al., 1990), particularly the biotinylated varieties (Brandt and Apkarian, 1992). Furthermore, computer systems for axonal reconstruction and analysis have become available (Capowski, 1989; Glaser et al., 1983; Glaser and Glaser, 1990).

Experimental and theoretical work performed mainly in the seventies has laid the groundwork for the analysis of the implications of axonal geometry for information pro-

cessing in the central nervous system (see Innocenti et al., 1994, for references). In addition, software specifically aimed at the simulation of axon potential propagation in axons has been described (see De Schutter, 1992, for references). In these programs, axons are modeled as sets of interconnected compartments with defined electrical properties; realistic action potentials can be recovered from the different compartments. Specific relations between the geometry of axonal arbors and their conduction properties could be predicted (e.g., Parnas, 1979; Lüscher and Shiner, 1990a,b; Manor et al., 1991a), some of which were experimentally verified.

The available simulators have drawbacks: (i) they require considerable computation time, which increases enormously with the complexity of the arbors to be analyzed; therefore, it is difficult to simulate the activity of multiple axons simultaneously; (ii) they are limited in their acceptance of realistic structural data, issued by anatomical analysis (De Schutter, 1992); and (iii) they require definition of biophysical parameters (in particular, capacitances and conductances and/or properties and distribution of ionic channels) for which few if any experimental data are available.

\* Corresponding author. Tel.: +41 21 692 51 35; Fax: +41 21 692 51 05.

Therefore, we have implemented a simpler event-driven simulation of axonal propagation based on a well-established relation between axon diameter and conduction velocity (Waxman and Bennett, 1972). The software, called Maxsim, avoids the difficulties mentioned above; it also facilitates the analysis of axonal morphology.

## 2. Program description

Maxsim is written in the language C (about 8000 lines) and runs under the Unix system. We used Sun Microsystems or Silicon Graphics™ workstations because their high graphic performance facilitates extensive analysis of the data obtained after 3-D reconstructions. Technical information and the executable program can be obtained free of charge by contacting the first author (Laurent.Tettoni@ia.unil.ch).

The program allows three sets of operations: pre-processing of data files, display of data in spatial or structural format, editing of axonal arbors and simulation of action potential propagation. Interactivity is ensured by pull-down menus, buttons, choice panels and dialog boxes selected using a pointing device. Fig. 1 illustrates a typical multi-window screen displayed during a Maxsim session.

The data obtained can be further analyzed either with Mathematica™ (Wolfram Research, Inc.) or Matlab™ (The Mathworks, Inc.) applications.

### 2.1. Data pre-processing

Maxsim imports morphological data obtained using the commercially available 3-D reconstruction software NeuroLucida™ (Microbrightfield, Inc.), based on the image-combining microscope concept (Glaser et al., 1983; Glaser and Glaser, 1990). NeuroLucida runs under MS-DOS or MS-Windows environments.

Each NeuroLucida file stores information on several objects (axonal segments, bifurcations called ‘nodes’, synaptic boutons, contour lines of sections, landmarks, etc.). It is organized as a serially ordered listing of graphical instructions describing all steps of the tracing procedure. Such a sequential format proved to be impractical for further use.

Therefore, when importing NeuroLucida files, Maxsim converts them into a binary tree, describing the topological and geometrical structure of the arbors. During this process the data are checked and the following possible acquisition errors are reported and can be corrected: (i) the coordinates of a bouton and those of the corresponding axonal segment

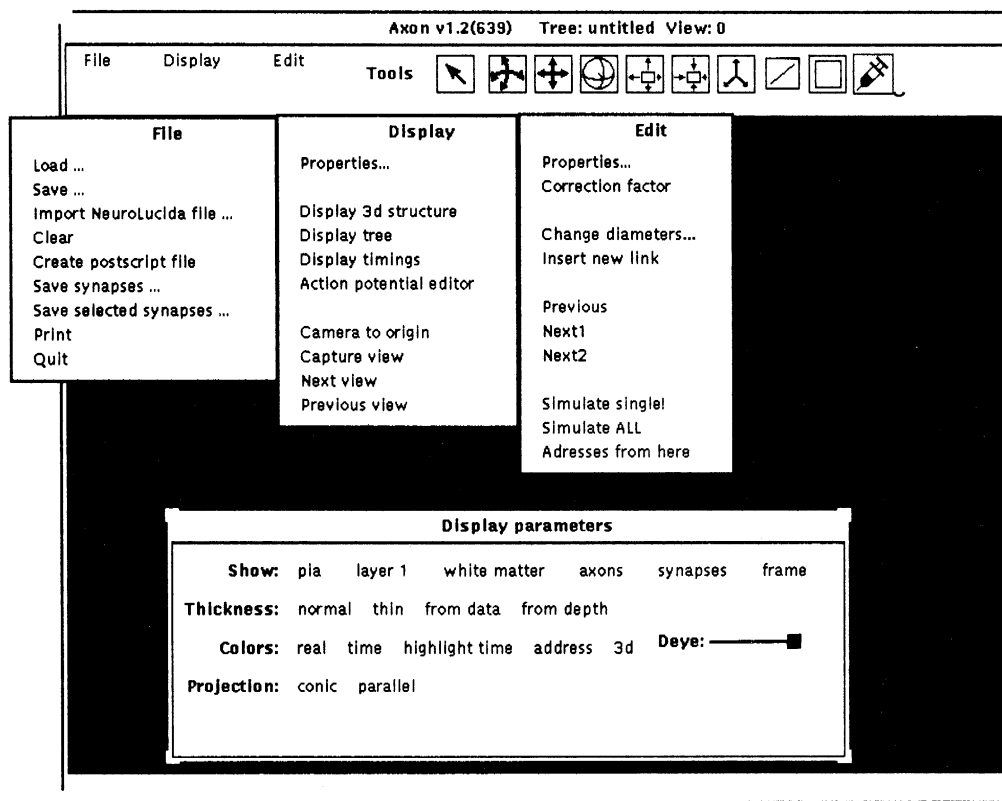


Fig. 1. Maxsim's menus. Main menu (top in main window) allows one to call submenus for managing files, displaying and editing options; tools allow (from left to right), selection of a point (in an axon or section outline),  $x/y$  translation and 3-D rotation of the object, zooming (in and out), 3-D rotation of frame of reference, selection of segments, boutons, or several points (each in a different axon). Submenus for file, display and edit are shown in middle windows; 'display parameters', is an example of dialog box used to define some of the parameters. The most important options are described in the text.

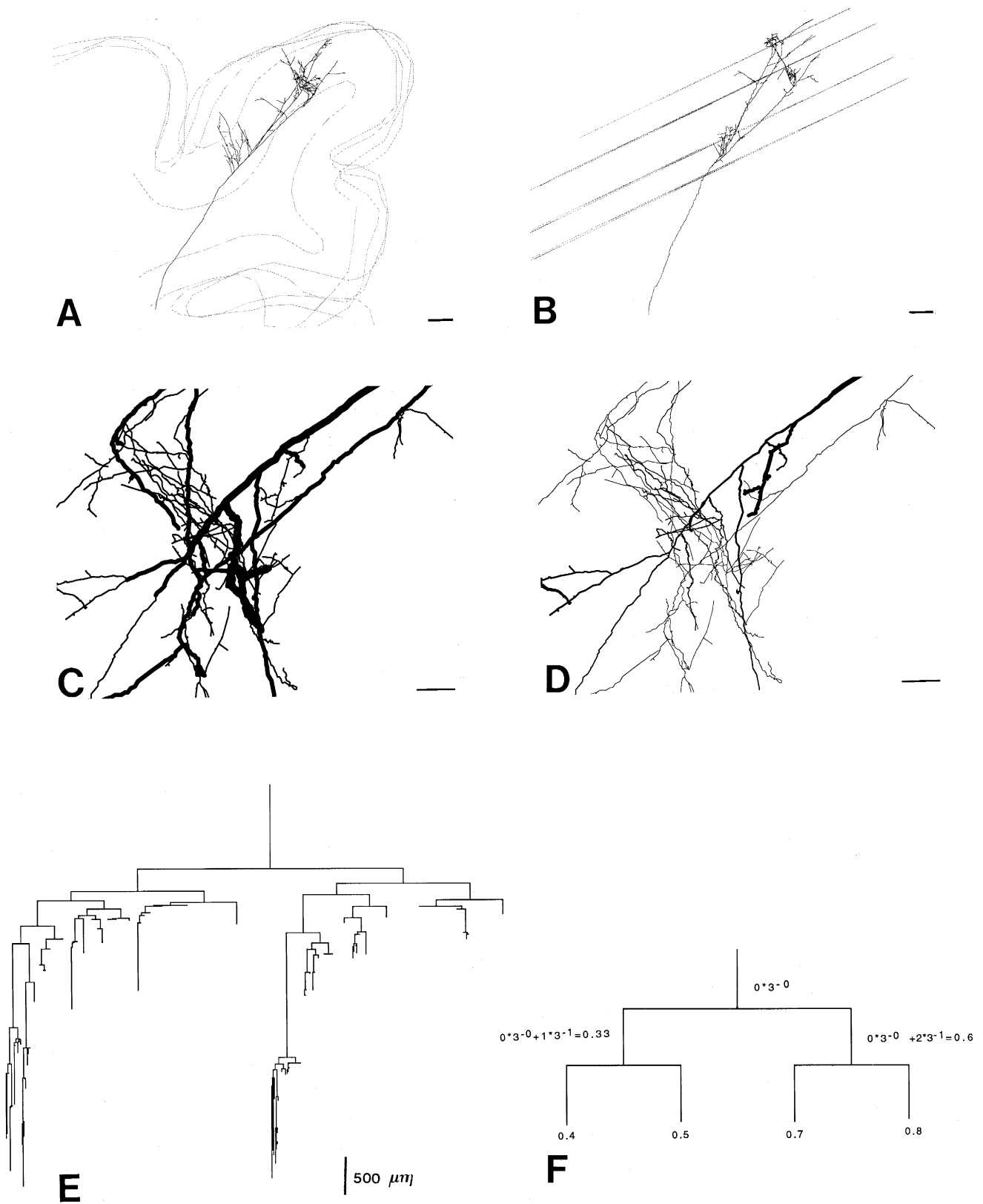


Fig. 2. Examples of display options. Top panels are front (A) and top (B) views of a serially reconstructed axon, viewed with the 'display parameters' option 'thin' (see Fig. 1) and contours of some of the sections which contain it. Middle panels show a detail of the same axon viewed with the option 'from data' (C; thickness is proportional to axon diameter) or 'from depth' (D; thickness is inversely proportional to distance from viewer). Bottom panels show examples of binary tree representation (E, called by 'display tree') and of computation of structural addresses described in the text (F). Scale bars are 500  $\mu\text{m}$ .

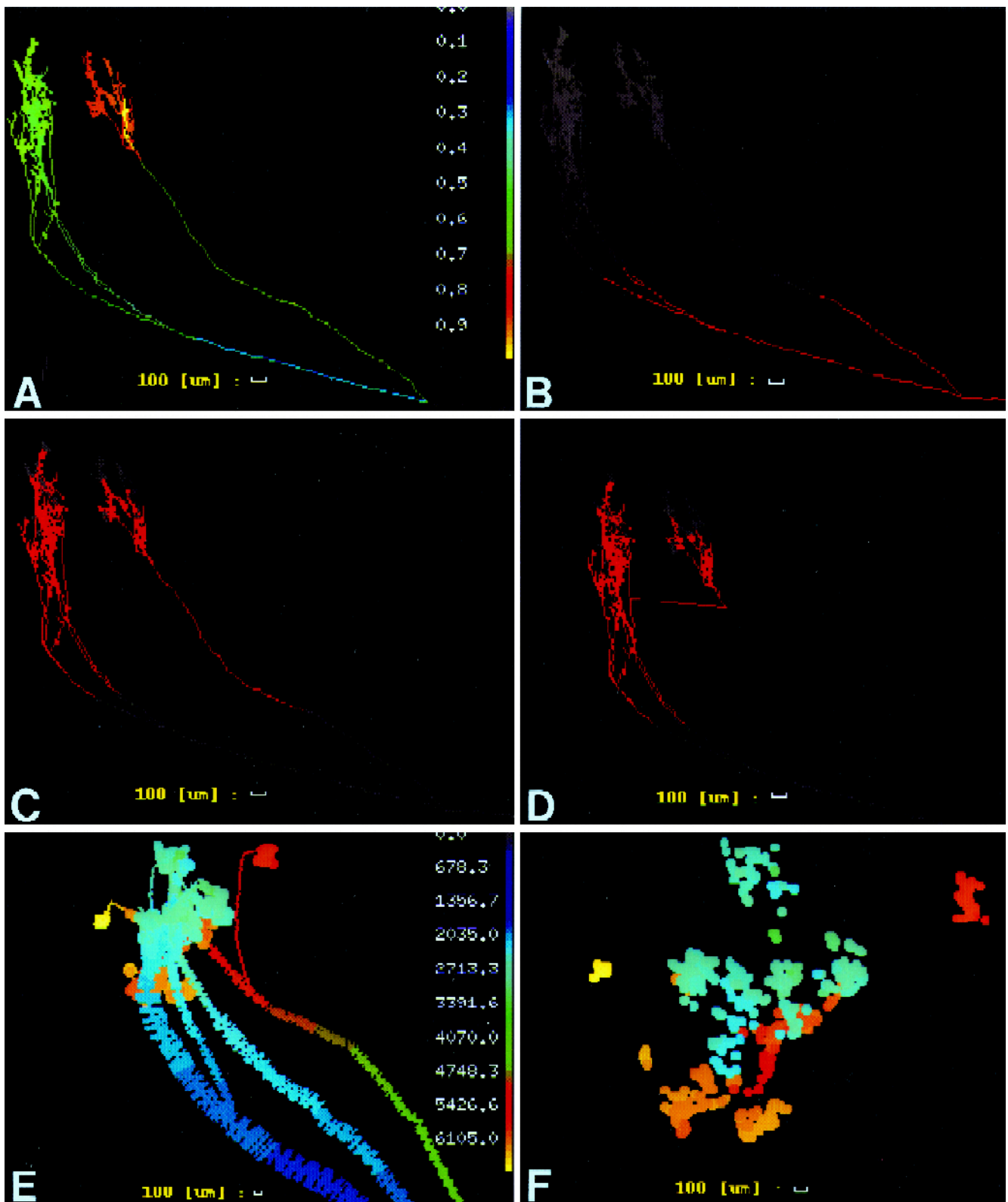


Fig. 3. (A) Example of visualization of structural addresses (values are color-coded), called by 'display parameters' option 'address' (Fig. 1). (B,C) Invasion of an arbor by an action potential as visualized by the option 'highlight'; the portion in red shows the depolarized part of the axon within a 300  $\mu$ s wide window 700  $\mu$ s (B) and 1000  $\mu$ s (C) after the initiation of the action potential. (D) 'Highlight' visualization as in C but on a modified version of the axon in which a long primary branch was replaced by a shorter, higher order branch obtained with 'Edit' option 'insert new link' (same window width and delay as above). Bottom panels (E,F) are isochrone representations of simultaneous action potential propagation in three axons shown in top view. The color range represents activation time in  $\mu$ s. In F, only the position of boutons (presumably synaptic boutons) is shown (enlarged). Thickness of axons was enlarged in the display and is not readable from scale bars. This was exaggerated in E and F.

most often differ by fractions of a micron. The simulation requires boutons to be actually connected to the tree. Thus, the bouton is connected to the nearest segment by inserting a supplementary node and a short virtual link of null diameter, and of infinite conduction velocity. When the required length of the virtual link exceeds a threshold (arbitrarily fixed to 1  $\mu\text{m}$ ), the user is alerted. (ii) Nodes from which more or less than two branches originate are displayed. (iii) Proximo-distal increases in axon diameter are reported. (iv) Correction factors can be introduced to compensate for tissue shrinkage (due to fixation) and compression (due to mounting and coverslipping). These factors are carried through the visualization procedures but they affect neither length measurements nor the simulation of spike propagation. The final structure can be filed in a new format. These files can be directly loaded for subsequent use.

When importing or loading data files, the total number of axons, their summed length, cytoplasmic volume and number of boutons are reported.

## 2.2. Display options

### 2.2.1. Spatial visualization

The reconstructed anatomical structures can be translated on the plane of view or can be 3-D rotated around any user-chosen axis using the mouse. A click-and-drag procedure is employed. 3-D rotation operates on a sphere centered on any point of the object and moving with it.

A triplet of colored cartesian axes can be introduced as a frame of reference. This frame can either be rotated independently or be frozen to any point of the reconstructed structure; when the latter is chosen, axes of rotation pass necessarily through the origin of the frame. This allows a user to choose a desired perspective, e.g. a top view at 90° from an initially defined ‘canonical’ starting position (Fig. 2A,B), different from that determined by the plane of histological cutting.

In order to render a perspective view of the reconstructed structures, the user can choose between parallel and conical projections onto the plane of view. In addition, points can be enlarged and highlighted inversely to distance from the observer (Fig. 2D).

Zoom-in and zoom-out functions allow one to vary magnification of the object.

In any view, selected parts of the reconstructed structures (i.e., section outlines, branches and boutons) can be visualized separately. Axonal segments can be represented with constant thickness or with thickness proportional to their real diameters (Fig. 2A,C).

Values of diameter or of structural address (defined below) of any segment in the arbor can be displayed using the mouse. Curvilinear length, defined as the total distance along the tree between any two selected points, can be read directly.

### 2.2.2. Structural visualization

Individual arbors can also be represented by binary trees (Fig. 2E,F). In this mode, the branching complexity of the arbor and the topological relations among branches can be appreciated.

We define a branch as a suite of axonal segments. Branches are located between two consecutive nodes, or between beginning or end of the axon and the nearest node. Each branch is assigned two characteristic numbers, ‘order’ in the tree and ‘structural address’.

The order of a branch is the number of nodes along the arbor from its origin to the branch.

The structural address  $V_p$  defines the topological location of a branch. It is computed as a function of the path followed along the tree to reach the branch from the beginning of the reconstruction. We propose the following equation:

$$V_p = \sum_{n=1}^N F(b_n) \cdot 3^{-n} \quad (1)$$

where  $n$  indicates order of branching in the tree,  $N$  is the largest order,  $F(b_n) = 1$  if branch  $b_n$  emerges from the ‘left’ side of a node and  $F(b_n) = 2$  if the branch  $b_n$  emerges from the ‘right’ side of a node. Left and right sides are purely conventional in the binary tree and do not correspond to the geometry of the arbor.

$V_p$  ranges between 0 and 1 (Fig. 2F). A color scale can be used to represent the whole range of structural addresses or a part of it in the 3-D visualization (Fig. 3A) or in the representation of the arbor as a binary tree.

## 2.3. Editing the morphology

Arbor structure can be modified to correct data acquisition errors or to conduct experiments on the relations between the geometry of an axon and its spatio-temporal pattern of activation.

Diameters of selected axonal branches can be modified. Any branch of the arbor can be replaced by a new branch with a user-chosen diameter, which can be grafted at a different location in the tree through a newly created node (Fig. 3D).

## 2.4. Simulation of action potential propagation

A single action potential can be initiated anywhere in an arbor and is conducted proximo-distally.

The simulation of action potential propagation is based on the following assumptions. (i) Each axon consists of cylindrical segments whose length are determined at tracing; segments have homogeneous conduction properties, defined by their diameter and length. (ii) Velocity of action potential propagation depends on diameter and remains constant along a segment.

The relation between conduction velocity  $V_c$  and axon diameter  $D$  of the fiber (in  $\mu\text{m}$ ; inclusive of myelin sheath, see below) is (Waxman and Bennett, 1972):

$$V_c = 5.5D [\text{m/s}] \quad (2)$$

This relation applies to central myelinated axons and takes into account the influence of internodal spacing (Brill et al., 1977). It requires definition of the fiber diameter (i.e. inclusive of myelin) whereas available tracers reveal axoplasm, and was thus replaced by:

$$V_c = (5.5/g)d [\text{m/s}] \quad (3)$$

where  $g$  is the ratio between axoplasm diameter ( $d$ , as optically measured during tracing) to fiber diameter ( $D$ , including the myelin sheath, as can be measured from electron microscopic studies). The default value of  $g$  is 0.77 (Waxman and Swadlow, 1976), but it can be modified by the user.

Therefore, the delay  $\partial t$  introduced by a segment of length  $L$  is:

$$\partial t = L/V_c [\mu\text{s}] \quad (4)$$

Action potentials may slow down at nodes, depending on the geometrical ratio  $g_r$  computed from the diameters of the parent branch  $d_p$  and the daughter branches  $d_{d1}$  and  $d_{d2}$ , according to the following equation (Goldstein, 1978):

$$g_r = \frac{d_{d1}^{3/2} + d_{d2}^{3/2}}{d_p^{3/2}} \quad (5)$$

Manor et al. (1991b) performed a theoretical study of delays introduced by nodes with  $g_r \neq 1$ , in non-myelinated axons. They found a relation between  $g_r$  and  $\partial t$  that can be approximated in the range ( $0.5 \leq g_r \leq 2.0$ ) by a linear equation. This range matches values of  $g_r$  found in cat callosal axons. The action potential leads 0.03 ms if  $g_r$  equals 0.5, and lags 0.06 ms if  $g_r$  equals 2.0. Maxsim uses the following rule:

$$\partial t = 0.06(g_r - 1) \quad (6)$$

The delay introduced by closely spaced nodes is treated by Maxsim as the sum of the individual delays although nonlinearities have been postulated by theoretical work (Manor et al., 1991b).

Unfortunately, delays at nodes strongly depend on a number of factors including the ionic conductances at the node, temperature, and clearance of extracellular  $\text{K}^+$  (Manor et al., 1991b), for which little if any experimental information is available. Moreover, it is not certain that this relation also applies to nodes of myelinated axons. Therefore, the introduction of delays at nodes by Eq. 6 is disabled by default, and must be enabled by the user.

We did not take into account the possible variations in conduction induced by swellings located at branching points or along branches, for which theoretical data are nevertheless available (Lüscher and Shiner, 1990a,b).

The action potential sequentially invades the segments defined during the reconstruction with delays caused by

the previous segments, dependent upon their diameter and length. The progression of the action potential can be visualized as a colored domain moving along the axon (Fig. 3B–D). The colored domain corresponds to a temporal window whose width and position can be adjusted within the total period of action potential propagation along the arbor, by moving two sliders. Frames representing the progression of the active domain can be individually saved and sequentially reloaded to generate an animation sequence.

An ‘isochrone’ representation of arrival times of action potential in different parts of the arbor can be displayed using a color spectrum; parts of the arbor becoming active at the same time acquire identical colors (Fig. 3E,F).

An adjustable wire frame can be used to select a subset of synaptic boutons. Each bouton is characterized by its spatial position, order of corresponding branch, structural address, curvilinear length from the beginning of the arbor and activation time. These data can be saved into a file suitable for further analysis by standard mathematical applications.

Multiple axons can be activated simultaneously. When this is done, delays can be added to the initiation of the action potential at the beginning of the reconstruction. This allows one to stagger the initiation of action potentials in different axons by delays corresponding to the conduction along the axonal segments situated between the anatomical origin and the beginning of the reconstruction.

### 3. Results

Maxsim was recently used in an extensive study of callosal axons interconnecting primary sensory visual cortices in the cat (Houzel et al., 1994; Innocenti et al., 1994).

Biocytin was extracellularly injected at the border between area 17 and 18. Axons labelled by anterograde transport were stained in 75  $\mu\text{m}$  thick frontal sections, and serially reconstructed. Procedures for histological visualization, 3-D reconstruction and analysis are detailed in the above-cited references. Only aspects directly related to the nature of rough data and their evaluation are described here, since they are directly relevant to the use of Maxsim.

Tissue deformation was evaluated from sets of stereotaxically placed microlesions, and shown to consist of two components: (i) A roughly isotropic shrinkage of about 35–40% observed after fixation, freezing and cutting. As it is difficult to determine whether shrinkage affects all cortical compartments in a similar fashion, and because activation profiles are unaffected when length and diameter are assumed to shrink proportionally, we did not apply any correction for this. (ii) A more severe compression occurs during the dehydration/coverslipping phase, reducing the section thickness to one third of its value at cutting, and causing all segments travelling along the  $z$ -axis to follow a wavy trajectory. This compression was compensated in the 3-D visualization, but not in length measure-

ments, since the trajectory of axons was faithfully followed during the reconstruction.

Our usage of the NeuroLucida system allowed accuracy of about 1  $\mu\text{m}$  on each axis. Stained processes were traced and measured at  $\times 1200$  magnification. Misalignments of axonal segments due to differential distortion of adjacent sections or coordinate mismatches were reasonably small (never more than 10  $\mu\text{m}$  and presumably random).

Axon diameters were ascribed to classes of 0.45  $\mu\text{m}$  width (0–0.44, 0.45–0.89  $\mu\text{m}$ , etc.), and later 0.26  $\mu\text{m}$  width (0–0.25, 0.26–0.51  $\mu\text{m}$ , etc.), which is close to the resolution of an optical microscope. Process diameter can be more accurately measured from on-line digitized images. Available CCD-video camera equipment allows reduction of the class width to 0.22  $\mu\text{m}$ .

Visual callosal axons having a trunk caliber in the range of those we reconstructed (0.65–2.02  $\mu\text{m}$ ) are myelinated in the cat (Berbel and Innocenti, 1988). A preliminary electron microscopic study (Aggoun-Zouaoui et al., unpublished) showed that (i) biocytin staining is restricted to the axoplasm; (ii)  $g$  ratios are close to 0.7 (as in rabbits; Waxman and Swadlow, 1976); (iii) axons seem to be myelinated up to their distal terminations. According to Waxman and Bennett (1972), a myelinated segment of 0.26  $\mu\text{m}$  diameter (i.e. corresponding to the narrowest class width) will have a conduction velocity of about 1.0 m/s, whereas a non-myelinated fiber of similar caliber will conduct at 1.1 m/s. Thus, if some preterminal branches (invariably around 0.25  $\mu\text{m}$  in diameter) were non-myelinated, conduction velocity would have been underestimated by less than 10% for those most distal portions.

The frequency distributions of activation delays (activation profiles) were computed for total boutons of an arbor and for separate clusters of boutons (Innocenti et al., 1994). Activation profiles for all the axons completely reconstructed from the midline returned latencies and mean conduction velocities very close to the electrophysiologically measured values available in the literature (discussed in Innocenti et al., 1994).

In an axon selected because of its complexity, we evaluated the influence of errors in the measurement of diameters on the simulation. All segments were assigned diameters at the lower or upper boundary of their class. This mimics a systematic error in diameter measurement equal to the half-width of the class. Error in activation time of the individual boutons did not exceed 9%. Non-systematic errors in diameter measurement tend to compensate and produce smaller errors.

#### 4. Discussion

Experimental results and simulations of action potential propagation have established that axons are more than simple wires connecting two points in the nervous system, but rather participate in information processing. In particu-

lar, axons can function as delay-lines which, in the auditory system, can be used to compute the position of a sound source (Carr and Konishi, 1990). Maxsim is designed to investigate this aspect of structure/function relationships in realistic representations of single or multiple axons, that can be obtained from 3-D computer-assisted reconstruction after anterograde filling.

In addition, axonal bifurcations can function as frequency filters of spike trains due to intermittent conduction failure in one of the branches (see Lüscher and Shiner, 1990a,b; Innocenti et al., 1994; for data and references). This aspect is not yet simulated by Maxsim.

A number of programs exist for simulation of the activity of individual neurons; they have been reviewed recently (De Schutter, 1992). Most of these programs are aimed at the study of computational properties of dendritic arbors. Their common goal is to provide detailed accounts of generation and conduction of potential along cables of defined geometrical and biophysical properties. Although some of these could also be used to simulate the propagation of action potentials in axons, their drawbacks were mentioned in Section 1.

We have tested Axontree, kindly made available to us by the authors (Manor et al., 1991a), for its capacity to simulate the speed of propagation of a single action potential as function of fiber diameter. The result was a square root function of fiber diameter, as measured in non-myelinated axons (Waxman and Bennett, 1972). However, for unknown reasons, it generated conduction velocities significantly below the experimental values. Therefore, Axontree appears to be unsuitable for the simulation of conduction in myelinated axons. Moreover, as stated by De Schutter (1992), importing realistic anatomical data is cumbersome.

The software described here addresses different questions. The focus is the spatio-temporal pattern of activity generated by one or more active axons. Therefore, Maxsim is designed for the analysis of anatomical data. These can be easily imported and handled. The program has a number of useful features which facilitate the qualitative analysis of axons. In addition, some quantitative investigations are possible with the program, others can be implemented on Maxsim-generated files using standard mathematical packages.

Precision of the results obtained with Maxsim, and their relevance, can be discussed. The software relies on time-consuming manual acquisition of anatomical data. This acquisition cannot be error free. Checking of anatomical files during importation identifies three common errors in the reconstruction procedures. Note that failure in connecting synaptic boutons to their parent segment can result from a deliberate tracing strategy which greatly accelerates data acquisition.

A crucial step in the tracing is the determination of axon diameters. The precision of this is limited first by the resolution of the optical microscope which is known to be

about 0.25  $\mu\text{m}$ . For the analysis of callosal axons this limit has the advantage of eliminating most or all non-myelinated axons (Berbel and Innocenti, 1988). For diameters above 0.25  $\mu\text{m}$ , axons were divided in classes multiple of 0.26  $\mu\text{m}$ . The width of these classes constitutes one limit in the precision of all the measurements which depend on the diameter. In the simulation, we evaluated the error to be less than 9%.

The accuracy of diameter as well as length estimates however also depends on other factors, including shrinkage, completeness of filling and cytoplasmic preservation as discussed elsewhere (Innocenti et al., 1994).

One important question concerns the degree of precision (or resolution) to be used in analyzing temporal patterns generated by Maxsim. The activation of the axon can be monitored by a temporal window of chosen width, moving centrifugally at the speed determined by diameter. We have used windows of 200–400  $\mu\text{s}$  corresponding to the duration of the depolarizing phase of the action potential and of the  $\text{Ca}^{2+}$  currents responsible for the release of neurotransmitters (Llinas, 1982). Shorter temporal windows are useful to analyze in detail the degree of synchronism in the activation of terminal boutons of an arbor. Auditory nuclei and nuclei which decode electric signals can extract information by analyzing synchronism in the  $\mu\text{s}$  range (Carr et al., 1986; Carr and Konishi, 1990). Recent electrophysiological and theoretical work stress the importance of synchronous activity of neural groups in cerebral cortex (Eckhorn et al., 1990; Engel et al., 1992) although in the ms range.

The accuracy of temporal information derived from a simplified model of action potential propagation such as implemented by Maxsim can be questioned. Indeed, propagation could depend on the presence of inhomogeneities in the biophysical properties of axons (as introduced by swellings, changes in the distribution of ionic channels, etc.) particularly at nodes (for references see Innocenti et al., 1994). Maxsim can simulate changes in conduction velocity due to changes of diameter at nodes, according to present hypotheses. However, further anatomical, physiological and biochemical investigations are required in order to identify the consequences of these inhomogeneities for local changes in conduction velocity or intermittent propagation of action potentials. More detailed information about the biophysical properties of myelinated axons would also be useful.

On the other hand, the simulations performed by Maxsim on the basis of the already available information may help to relate the temporal properties of the activity of individual neurons or of neuronal ensembles to the details of their underlying connectivity.

### Acknowledgements

Supported by European Training Programme in Brain and Behavioral Research Twinning grant 9185, Swiss Na-

tional Science Foundation grant 31-39707.93, and UNIL-EPFL funds. J-C.H. is the recipient of a 'Berthe Fouassier' fellowship of the 'Fondation de France'. We are grateful to Rudi Kraftsik for help with the computer work, Eric Bernardi for the illustrations and to Ann Gray for useful comments on the manuscript. We are very grateful to Dr. Manor for making Axontree available to us.

### References

- Berbel, P. and Innocenti, G.M. (1988) The development of the corpus callosum: a light and electron microscopic study, *J. Comp. Neurol.*, 276: 132–156.
- Brandt, H.M. and Apkarian, A.V. (1992) Biotin-dextran: a sensitive anterograde tracer for neuroanatomic studies in rat and monkey, *J. Neurosci. Methods*, 45: 35–40.
- Brill, M.H., Waxman, S.G., Moore, J.W. and Joyner, R.W. (1977) Conduction velocity in myelinated fibers: Computed dependence on internode distance, *J. Neurol. Neurosurg. Psychiatr.*, 40: 769–774.
- Capowski, J.J. (1989) *Computer Techniques in Neuroanatomy*, Plenum Press, New York.
- Carr, C.E., Heiligenberg, W. and Rose, G.J. (1986) A time-comparison circuit in the electric fish midbrain. I. Behavior and physiology, *J. Neurosci.*, 6: 107–119.
- Carr, C.E. and Konishi, M. (1990) A circuit for detection of interaural time differences in the brainstem of the barn owl, *J. Neurosci.*, 10: 3227–3246.
- De Schutter, E. (1992) A consumer guide to neuronal modeling software, *Trends Neurosci.*, 15: 462–464.
- Eckhorn, R., Reitboeck, H.J., Arndt, M. and Dicke, P. (1990) Feature linking via synchronization among distributed assemblies: simulations of results from cat visual cortex, *Neural Comput.*, 2: 293–307.
- Engel, A.K., König, P., Kreiter, A.K., Schillen, T.B. and Singer, W. (1992) Temporal coding in the visual cortex: new vistas on integration in the nervous system, *Trends Neurosci.*, 15: 218–226.
- Gerfen, C.E. and Sawchenko, P.E. (1984) An anterograde neuroanatomical tracing method that shows detailed morphology of neurons, their axons, and terminals: immunohistochemical localization of axonally transported plant lectin, Phaseolus vulgaris leucoagglutinin, *Brain Res.*, 290: 219–238.
- Glaser, E.M., Tagamets, M., McMullen, N.T. and Van der Loos, H. (1983) The image-combining computer microscope – an interactive instrument for morphometry of the nervous system, *J. Neurosci. Methods*, 8: 17–32.
- Glaser, J.R. and Glaser, E.M. (1990) Neuron imaging with neuroLucida – A PC-based system for image combining microscopy, *Comput. Med. Imag. Graphics*, 14: 307–317.
- Goldstein, S.S. (1978) Models of Conduction in Nonuniform Axons. In S.G. Waxman (Ed.), *Physiology and Pathobiology of Axons*, Raven Press, New York, pp. 227–236.
- Houzel, J.C., Milleret, C. and Innocenti, G.M. (1994) Morphology of callosal axons interconnecting areas 17 and 18 of the cat, *Eur. J. Neurosci.*, 6: 898–917.
- Innocenti, G.M., Lehmann, P. and Houzel, J.C. (1994) Computational structure of visual callosal axons, *Eur. J. Neurosci.*, 6: 918–935.
- King, M.A., Louis, P.M., Hunter, B.E. and Walker, D.W. (1989) Biotin: a versatile neuroanatomical tract-tracing alternative, *Brain Res.*, 497: 361–367.
- Llinas, R.R. (1982) Calcium in synaptic transmission, *Sci. Am.*, 247: 56–65.
- Lüscher, H.R. and Shiner, J.S. (1990a) Computation of action potential

- propagation and presynaptic bouton activation in terminal arborizations of different geometries, *Biophys. J.*, 58: 1377–1388.
- Lüscher, H.R. and Shiner, J.S. (1990b) Simulation of action potential propagation in complex terminal arborizations, *Biophys. J.*, 58: 1389–1399.
- Manor, Y., Gonczarowski, J. and Segev, I. (1991a) Propagation of action potentials along complex axonal trees, *Biophys. J.*, 60: 1411–1423.
- Manor, Y., Koch, C. and Segev, I. (1991b) Effects of geometrical irregularities on propagation delay in axonal trees, *Biophys. J.*, 60: 1424–1437.
- Parnas, I. (1979) Propagation in nonuniform neurites: form and function in axons. In F.O. Schmitt and F.G. Worden (Eds.), *The Neurosciences*, MIT Press, Cambridge, pp. 499–512.
- Schmued, L.C., Kyriakidis, K. and Heimer, L. (1990) In vivo anterograde and retrograde axonal transport of the fluorescent rhodamine-dextran-amine, Fluoro-Ruby, within the CNS, *Brain Res.*, 526: 127–134.
- Waxman, S.G. and Bennett, M.V.L. (1972) Relative conduction velocities of small myelinated and non-myelinated fibres in the central nervous system, *Nature*, 238: 217–219.
- Waxman, S.G. and Swadlow, H.A. (1976) Ultrastructure of visual callosal axons in the rabbit, *Exp. Neurol.*, 53: 115–127.